INTERNATIONAL JOURNAL OF INTEGRATED ENGINEERING
ISSN: 2229-838X e-ISSN: 2600-7916

IJIE

Vol. 17 No. 6 (2025) 210-223
https://publisher.uthm.edu.my/ojs/index.php/ijie

Effect of Annealing Time on the Properties of Interstacked Magnesium-Doped Cu_2O/Cuo Thin Films

Fatin N. Afiqah[1], N Nisha Razalli[1], M. Zamzuri[1]*, M Mahyiddin[2], A.F Aiman[2], H Jaafar[2], F Mohamad[3], P L Khoo[4], M Izaki[5]

[1] *Faculty of Mechanical Engineering Technology, Universiti Malaysia Perlis (UniMAP), Pauh Putra Campus, 02600 Arau, Perlis, MALAYSIA*
[2] *Faculty of Electronic Engineering Technology, Universiti Malaysia Perlis (UniMAP), Pauh Putra Campus, 02600 Arau, Perlis, MALAYSIA*
[3] *Faculty of Electrical & Electronic Engineering, University Tun Hussein Onn Malaysia, 86400, Parit Raja, Batu Pahat, Johor, MALAYSIA*
[4] *Department of Mechanical Engineering, Toyohashi University of Technology, 1-1 Hibari Gaoka, Tempaku, Toyohashi, Aichi 441-8580, JAPAN*
[5] *Social Cooperation Center, Nara Women's University, Kitauoya-Higashimachi, Nara 630-8506, JAPAN*

*Corresponding Author: mzamzuri@unimap.edu.my
DOI: https://doi.org/10.30880/ijie.2025.17.06.017

Article Info

Received: 30 May 2025
Accepted: 16 September 2025
Available online: 30 December 2025

Keywords

Cu_2O, electrodeposition, annealing effect, photovoltaic devices, Mg doping

Abstract

Cuprous oxide (Cu_2O) is an attractive candidate for cost-effective and sustainable solar cells due to its direct bandgap and natural p-type conductivity. We report on the investigation of the effect of annealing time on the morphological, optical, structural and electrical properties of interstacked Mg:Cu_2O/CuO thin films. The thin films were synthesized using the electrodeposition method of Cu_2O layers on indium tin oxide (ITO) substrate followed by annealing at 300°C for different durations (60, 120, 180, and 240 minutes). As a result, we found that by increasing annealing time up to 180 minutes, the formation of CuO thin film increases, surpassing the Cu_2O as revealed by X-ray diffraction (XRD) analysis. The band gaps remain constant at 2.5 eV, irrespective of annealing time. Carrier concentration increased upon the annealing time, reaching a value of 2.255×10^{21} ($/cm^3$), which demonstrates the complementary effects of magnesium (Mg) doping and annealing time.

1. Introduction

Cuprous oxide (Cu_2O) is a promising material for solar cell applications because of its inherent p-type semiconducting properties, abundance on Earth, and appropriate bandgap for solar energy conversion [1]. Its fabrication can be achieved through a variety of cost-effective and scalable techniques, making it a viable alternative to more expensive or less sustainable photovoltaic materials. Common methods include thermal evaporation and electrodeposition, which are widely employed due to their simplicity and ability to produce uniform thin films [2].

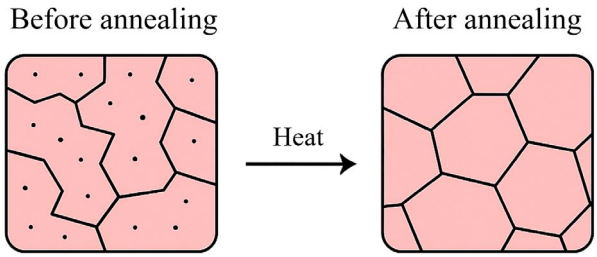

Fig. 1 *Schematic illustration of the annealing process showing grain structure transformation. Annealing promotes grain growth and uniformity through recrystallization and the reduction of structural defects*

Additionally, several other deposition techniques have been employed to fabricate Cu_2O thin films with tailored properties. High-energy laser pulses are used in pulsed laser deposition (PLD) to ablate a target material, allowing for the controlled growth of crystalline, high-purity CuO films [3]. Low-cost synthesis and accurate compositional tuning are made possible by the solution-based method known as sol-gel processing [4]. Chemical vapor deposition (CVD), which is perfect for complex surface geometries, uses chemical reactions in the vapor phase to create dense, conformal films [5]. Rapid and scalable film fabrication is made possible by spray pyrolysis, which uses atomized precursor solutions deposited onto heated substrates [6]. These diverse synthesis techniques enable precise control over the morphology, crystallinity, and thickness of Cu_2O films, enhancing their suitability for photovoltaic device applications. Perovskite solar cells (PSCs) and other photovoltaic devices frequently utilize Cu_2O as a hole transport material to enhance power conversion efficiency (PCE) and enable effective charge extraction [7]. Despite its potential, issues like low electrical conductivity and high charge carrier recombination rates must be resolved to improve its performance [8]. Various research has been done to determine the most effective methods for optimizing the characteristics of Cu_2O-based solar cells, and it is proven that doping techniques and annealing are among the best strategies.

Introducing impurity levels through doping can improve charge carrier mobility and decrease recombination by facilitating the separation of photogenerated electron-hole pairs. For instance, Lu Wang et. al. have demonstrated that surface Cu doping in perovskite structures lowers surface energy and inhibits oxidation, improving phase stability and lowering electron accumulation [9]. Besides that, Akshai Shyam et al have proven that Mg doping has a significant positive effect on both electrical (hole concentration) and optoelectronic (photocurrent, responsivity, detectivity) properties of $CuCrO_2$ thin films. The 2% Mg-doped $CuCrO_2$ film of their research exhibited a maximum hole concentration of approximately 10^{19} cm^{-3}, which is a substantial improvement in p-type conductivity [10]. It has been demonstrated that magnesium doping increases stability and efficiency in a variety of photovoltaic materials, including ZnO and TiO_2. It improves photovoltaic performance by expanding absorption ranges, decreasing band gaps, and improving the optical and morphological characteristics of electron transport thin films [11-13].

Apart from doping, annealing is also considered among the best strategies for improving the performance of Cu_2O-based photovoltaic devices due to its ability to enhance the morphology and crystal structure of Cu_2O thin films as well as reduce defects. Fig. 1 shows a Schematic illustration of the annealing process showing grain structure transformation. Annealing promotes grain growth and uniformity through recrystallization and the reduction of structural defects. In a study on n-TiO_2/ZnO thin films, for instance, films with high crystallinity and homogeneous morphology were produced by annealing at 500 °C for two hours [14]. This is crucial for lowering the electron-hole recombination rate. In Au-Cu_2O-CuO nanocomposites, annealing results in a notable increase in the size of the nanostructures, which helps to improve the photocatalytic capabilities [15]. Annealing also contributes to better electron-hole pair separation, which is vital to raising photovoltaic devices' efficiency. Annealing aided in the creation of Z-scheme heterojunction structures in the Cu_2O-WO_3 study, improving the separation of photogenically generated electrons and holes [16].

In contrast to previous studies, the present work specifically investigates the effect of annealing duration on interstacked Mg-doped Cu_2O/CuO thin films synthesized via the electrodeposition method. Our previous study utilized electrodeposition for fabricating Mg-doped Cu_2O films. However, their study was limited to as-deposited samples, without exploring post-deposition thermal treatment. Chinmoy Rajak et al. conducted annealing of sputtered copper films at various temperatures, focusing on a fixed duration of 1 hour and excluding any doping variation. Naveen Kumar et al. explored Na/Co co-doped Cu_2O films prepared via sol-gel techniques with high-temperature annealing, yet the specific annealing times were not addressed. Wen-len Lee et al. investigated the effects of annealing time using the SILAR method, although Mg doping was outside the scope of their study. Uniquely, this research integrates electrodeposition, Mg doping, interstacked Cu_2O/CuO architecture, and controlled variation of annealing time, providing valuable insights into the thermal influence on microstructural and optical properties.

Int. Journal of Integrated Engineering Vol. 17 No. 6 (2025) p. 210-223

This study demonstrated the synthesis of interstacked Mg-doped Cu_2O/CuO thin films by electrodeposition of Mg-doped Cu_2O on the ITO glass substrate, followed by annealing at 300°C for 60, 120, 180, and 240 minutes. The effect of annealing time on the structural, optical, morphological, and electrical properties was investigated. Our research shows that controlling the annealing parameter is essential to achieving the best possible physical characteristics for the produced thin films. In this report, the corresponding obtained results are discussed.

2. Methodology

2.1 Thin Film Deposition

Fig. 2 displays the flowchart of the methodology for this study. Potentiostatic electrodeposition of the Cu_2O thin film was performed with a potentiostat/galvanostat (Hokuto Denko HABF-501A, Hokuto Denko Corporation). A platinum plate as a counter electrode and an indium tin oxide substrate (ITO, sheet resistance of about 10 mΩ) measuring 20 mm by 10 mm comprise a traditional two-electrode system. The distance between the sample and the counter electrode was about 1 cm. A controlled temperature water bath was used to maintain the electrolyte's temperature at 40°C throughout the deposition process. During the experiments, there was no stirring.

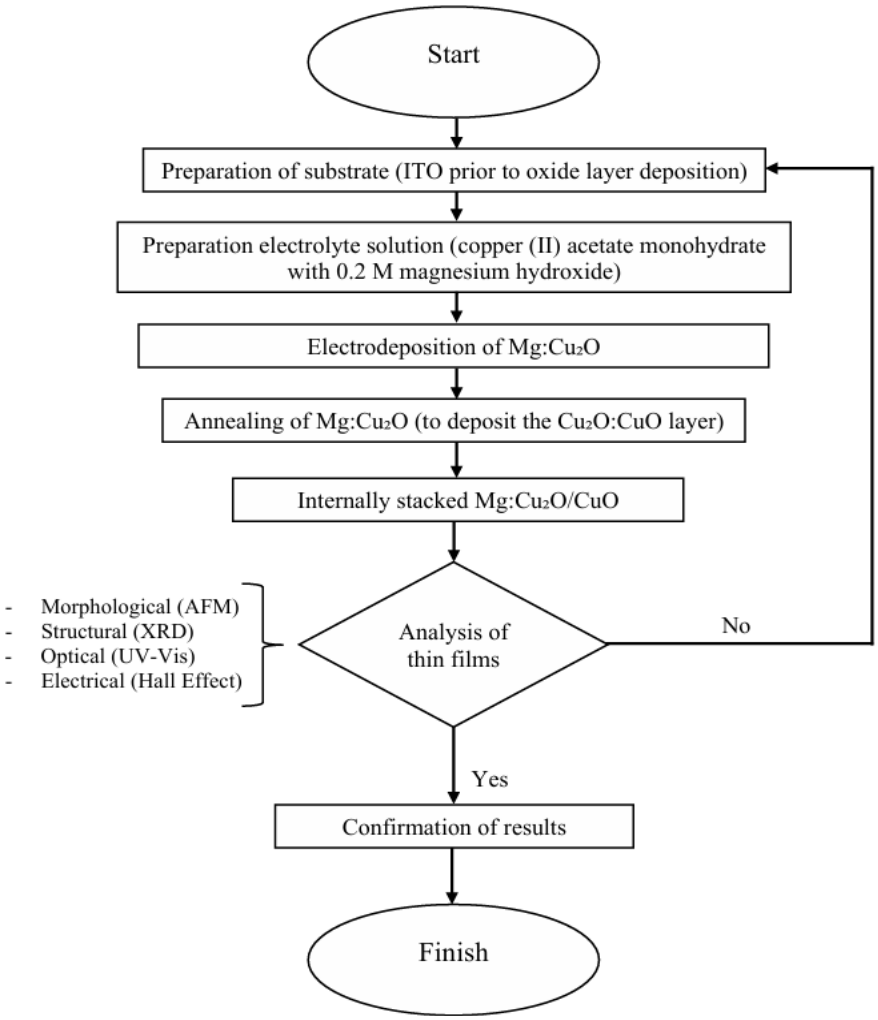

Fig. 2 *Flowchart of the methodology*

2.2 Preparation of Substrate

In order to remove any surface contaminations, the ITO substrates were immersed in acetone (CH_3COCH_3) for 3 minutes. The ITO substrate is then rinsed using ultra-pure water and blow-dried using a rubber hand blower. A Teflon tape is used to separate the area to be deposited (10 mm x 10 mm) and the non-deposited area (10 mm x 10 mm). Next, the ITO substrate is set up for an alkali pre-treatment as shown in Fig. 3. The substrate and a counter electrode are immersed in sodium hydroxide (NaOH) solution and connected to a potentiostat. The potentiostat was set to -200 mA and immersed for 1 minute.

2.3 Fabrication of Cu_2O Thin Film

Fig. 4 displays the schematic diagram of the electrodeposition of Cu_2O thin film. Copper (II) acetate, $Cu(COOCH_3)_2$ alkaline aqueous solution was used to electrochemically deposit the Cu_2O thin films. The electrolyte was prepared by dissolving 0.4 M of copper (II) acetate 29 monohydrate, $Cu(COOCH_3)_2{\cdot}H_2O$ powder, 3 M of lactic acid, $CH_3CH(OH)COOH$, and 500 ml of ultrapure water (UPW) at room temperature with 3.7 M of potassium hydroxide, KOH crystal. A pH of 12.5 was adjusted using KOH crystals. The solution is then added with 95% pure magnesium hydroxide to formulate a doping concentration of 0.2 M. The deposition was carried out potentiostatically at a constant voltage of 1V with a current input of 2 mA for 3 minutes. The solution was kept at 44 °C throughout the electrodeposition process by using a temperature-controlled water bath. Following a thorough rinse with distilled water, the electrodeposited samples were left to dry naturally at room temperature.

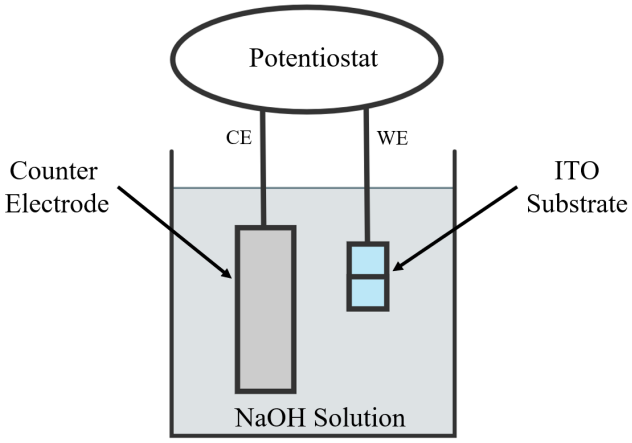

Fig. 3 *The schematic diagram of the alkali pre-treatment setup*

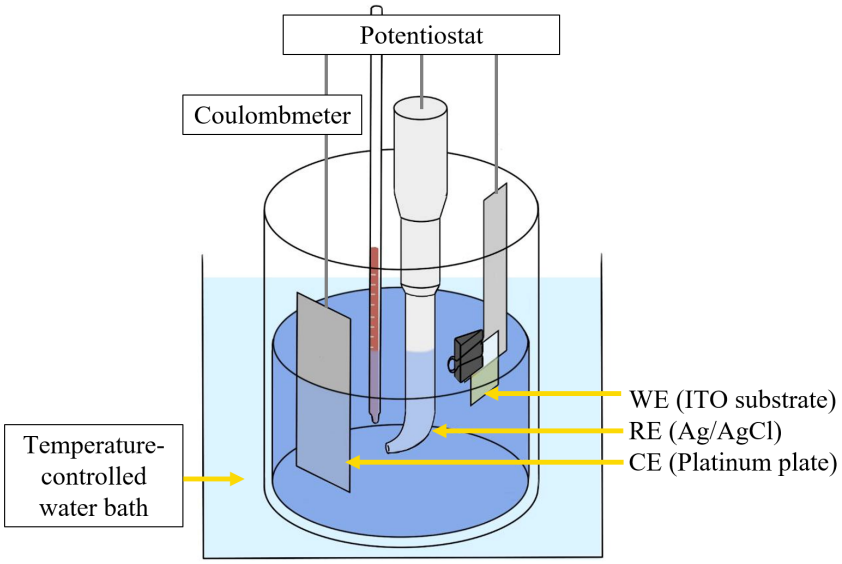

Fig. 4 *The schematic diagram of the electrodeposition of Cu_2O thin film*

Int. Journal of Integrated Engineering Vol. 17 No. 6 (2025) p. 210-223

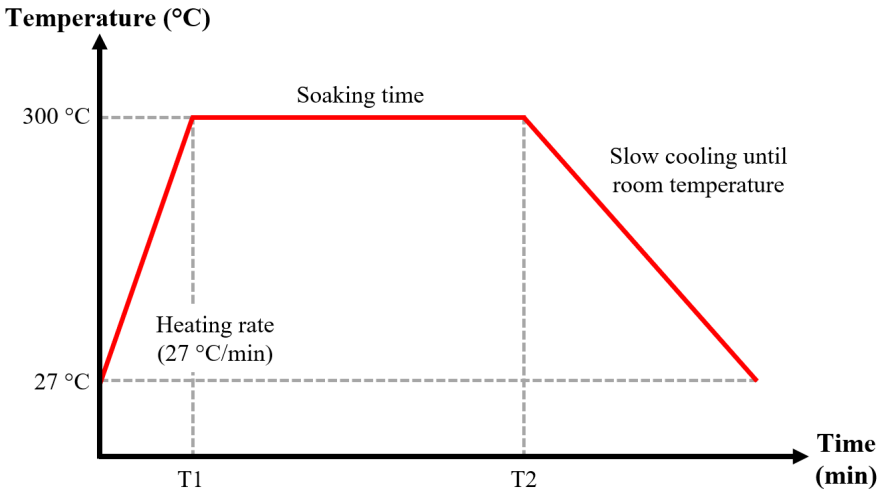

Fig. 5 *The annealing temperature profile*

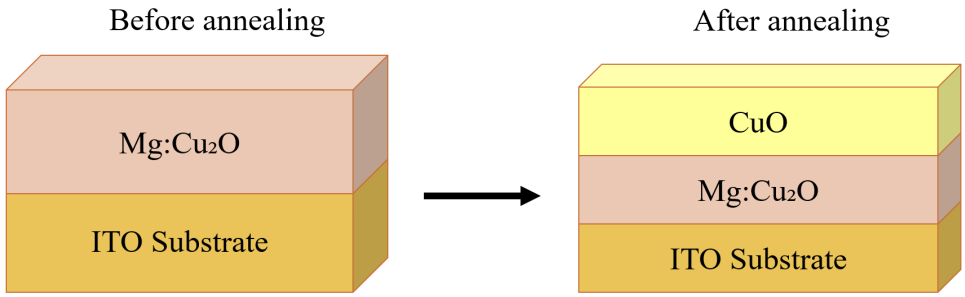

Fig. 6 *Schematic illustration of the cell configuration of Mg:Cu_2O/CuO thin film before and after annealing*

2.4 Annealing of Cu_2O Thin film

Fig. 5 shows the annealing temperature profile. Following the electrodeposition process, the Cu_2O layer is annealed in a mini lamp annealer (Mila 5000, Ulvac Malaysia) to increase grain size and create the CuO layer in the Cu_2O thin film. The heating process begins at 27 ºC room temperature, and the annealer's heating rate was adjusted to 27 °C/min. A temperature of 300 °C was maintained as the annealing temperature, T setting. The times used for annealing are 60, 120, 180, and 240 minutes. After that, the sample is left to cool in the furnace until it reaches room temperature. Figure 3.8 shows the setting of the annealing parameters for Cu_2O thin film.

2.5 Materials and Device Characterization

The surface morphology and microstructure of the prepared nanostructures were examined using an Atomic Force Microscope (connected to an SPA400 Soundproof Housing). The scan size in the range of 3 µ to 5 µ with 0° to 45° for light angle and 20° to 45° for the view angle were used for this analysis. The orientation and crystal structure of interstacked Mg:Cu_2O/CuO thin film were determined using an X-ray Diffractometer (XRD BRUKER D2 PHASER) with monochromated $CuK\alpha_1$ radiation (γ = 1.54056 Å) operated at 20 KV and a scan range of 20° to 80°. The optical properties were evaluated using ultraviolet and visible absorption spectroscopy (PerkinELMER LAMBDA 950 Series). The range, with reference to the air, was set between 200 and 800 µm. Electrical properties of the thin film were observed by Hall Effect Measurement (ECOPIA HT55T3) with a current of 1 mA, and a diameter of 0.1 µm to measure the mobility carrier, resistivity, and carrier concentration.

3. Result

3.1 Modification of internally stacked Mg:Cu_2O/CuO Thin Film

Fig. 6 presents a schematic illustration of the Mg-doped Cu_2O (Mg:Cu_2O) thin film structure on an ITO glass substrate before and after annealing. Prior to annealing, the as-deposited film comprises a single-phase Mg:Cu_2O layer directly on the ITO substrate. This structure represents the initial state of the electrodeposited film with

limited oxidation. However, after the annealing process, thermal treatment induces partial oxidation of Cu^{+} to Cu^{2+}, resulting in the formation of a CuO phase on the surface or within the film matrix. This transition leads to the development of a bilayer configuration denoted as Mg:Cu_2O/CuO. The presence of both Cu_2O and CuO phases in the annealed film is crucial for modifying the electrical and optical properties of the device, potentially enhancing charge separation and transport in optoelectronic applications.

3.2 Appearance of Interstacked Mg:Cu_2O/CuO Thin Films

Fig. 7 shows the physical appearance of the Mg:Cu_2O thin films on ITO substrate glass following annealing at various annealing times. The electrodeposited Mg-doped Cu_2O (Mg:Cu_2O) thin films were annealed at a constant temperature of 300°C for 60, 120, 180, and 240 minutes in air. At 60 minutes, the surface appears relatively uniform and smooth, indicating a thin, compact layer with minimal oxidation. As the annealing time increases to 120 minutes and 180 minutes, the films become progressively more non-uniform in brightness and texture. This change may suggest partial grain growth, increased surface roughness, or the onset of CuO formation. By 240 minutes, the film exhibits a more diffuse or hazy appearance, likely caused by further oxidation, coarsening of the surface, or the formation of secondary phases, such as CuO becoming dominant over Cu_2O. Further identification of material changes over time can be observed through the intensity and position of peaks in the X-ray Diffraction (XRD) patterns. As annealing time increases, changes in peak intensity, sharpness, and possible peak shifts indicate modifications in crystallinity, phase composition, and grain size.

3.3 Morphology Properties of Interstacked Mg:Cu_2O/CuO Thin films

Fig. 8 displays the 3D Atomic Force Microscopy (AFM) images of interstacked Mg:Cu_2O/CuO thin films annealed at 60, 120, 180, and 240 minutes. It is evident that the Cu_2O grains changed significantly with various annealing times. The annealed Cu_2O crystal shows a textured surface with three-sided pyramidal grains. Sample annealed for 60 min revealed the structure of smaller grains of Cu_2O with an average grain size of 305.3 nm. Then, as the annealing time increased, the grains became larger at 120 minutes with an average grain size of 408.30 nm. The coalescence between larger grains was seen over the Cu_2O surface. Research confirms that at 300°C, CuO grains begin to form on top of the Cu_2O layer at 300°C which suggests that the phase transition from Cu_2O to CuO is facilitated by higher temperatures, which also contributes to the grain size change [17-18]. However, as the annealing time reached 180 and 240 minutes, a smaller and more compact pyramid-like structure was obtained. This is highly due to prolonged annealing, which then may cause phase changes or the emergence of new phases, which could lead to smaller grain sizes as new nucleation sites develop [19].

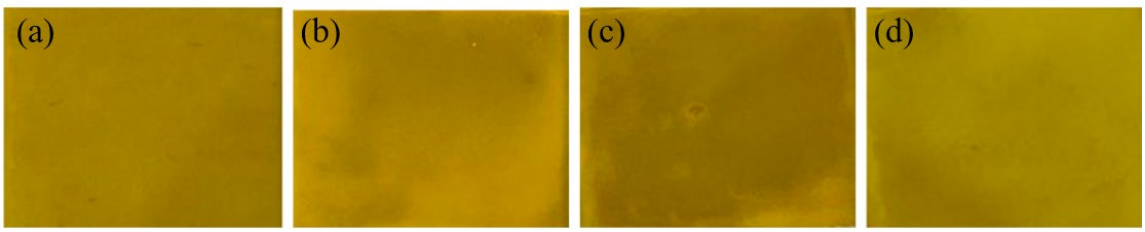

Fig. 7 *The appearance of Mg:Cu_2O thin film annealed at (a) 60 minutes; (b) 120 minutes; (c) 180 minutes; and (d) 240 minutes*

Int. Journal of Integrated Engineering Vol. 17 No. 6 (2025) p. 210-223

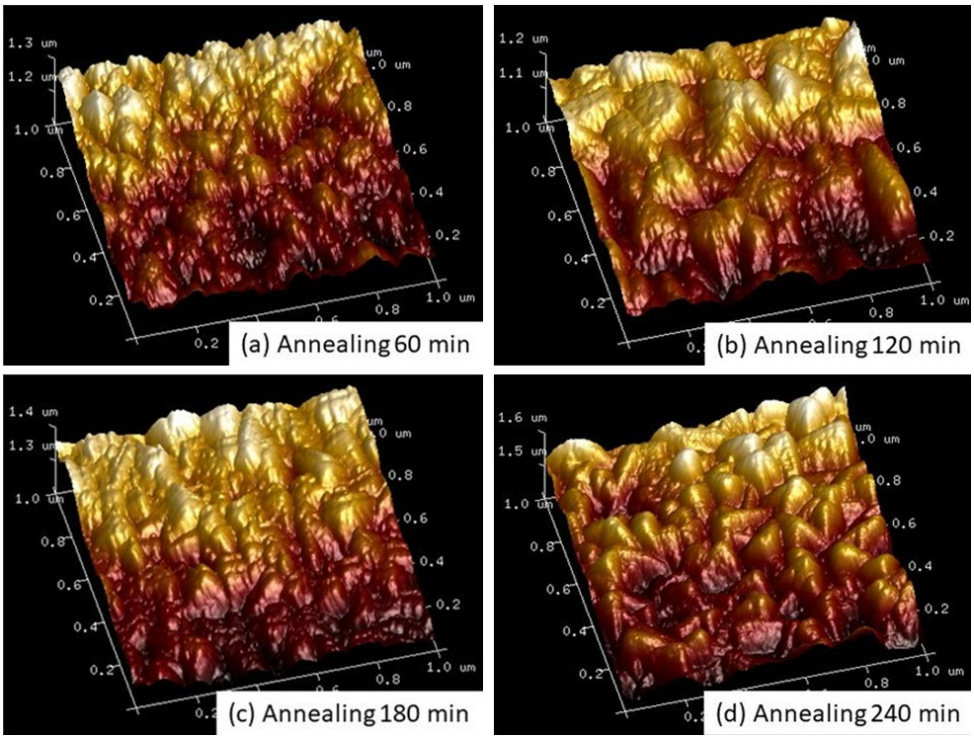

Fig. 8 *3-Dimensional AFM images of the interstacked Mg:Cu_2O/CuO thin films*

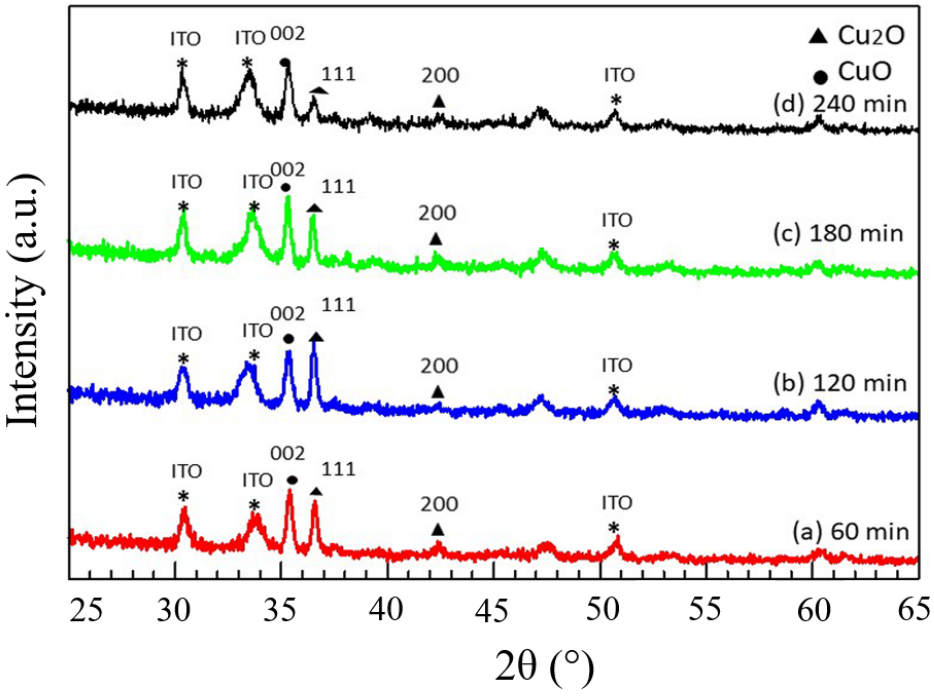

Fig. 9 *XRD diffraction pattern of the interstacked Mg:Cu_2O/CuO thin films*

3.4 Structural Properties of Interstacked Mg:Cu_2O/CuO Thin Films

The crystal structure and orientation of interstacked Mg:Cu_2O/CuO thin films were investigated using X-ray diffraction (XRD). Fig. 9 shows the XRD patterns for the deposited Cu_2O thin film at various annealing times of 60, 120, 180, and 240 min. At 36.4° of the diffraction peak, the deposited Cu_2O thin films displayed orientation indexed

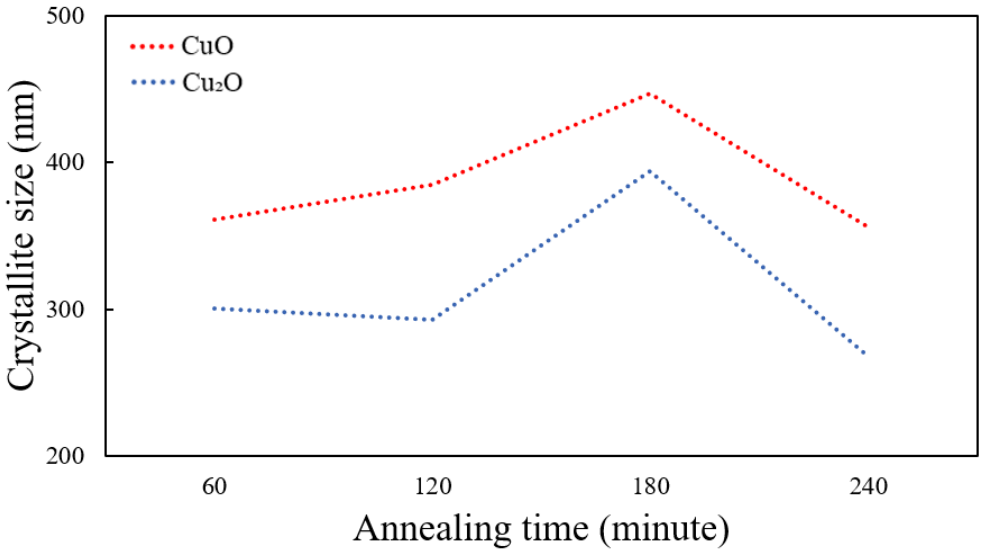

Fig. 10 *Crystallite size versus annealing time of the interstacked Mg:Cu_2O/CuO thin films*

to (111) as well as extra peaks, particularly the (200) reflection of the Cu_2O thin-film diffraction peak at 43.0°. The cubic pattern corresponded to the Cu_2O orientation (PDF 01-071-3645). The CuO peak at 35.5° of the diffraction peak was indexed to (002), while CuO orientation corresponded to the monoclinic lattice pattern (PDF 00-048-1548). No additional peaks were observed with respect to magnesium, indicating the absence of any signs of a secondary phase. This is anticipated due to the small amount of Mg added to the copper (II) acetate solution. The doping of Mg is intended to substitute Cu2+ ions with Mg2+ ions without producing any new phase [20]. According to Marina et al, the temperature for the formation of CuO grains could start at approximately 300 °C [21]. From Fig. 9, it can be seen that peak (111) Cu_2O thin film is almost constant as the annealing time increases, but starts to decrease at 180 and 240 minutes. This is due to the excessive formation of CuO resulting from the oxidation of the Cu_2O thin film. According to Lee et al., annealing copper oxide films at 300 °C can cause Cu_2O to gradually transition to CuO due to changes in the crystal structure as the annealing time increases, which can significantly impact the material's properties [22].

Fig. 10 displays the crystallite size versus annealing time of the interstacked Mg:Cu_2O/CuO thin films at various annealing times. The crystallite size was estimated from the XRD peaks using the Scherrer equation, which reflects the size of coherently diffracting domains, which are the internal regions within grains that have uniform lattice orientation. The Scherrer's equation employed to estimate the crystallite size, uses the following equation:

$$D = K\lambda/\beta \cos \theta \quad (1)$$

where D is the crystallite size, λ the X-ray wavelength, β is the full width at half-maximum (FWHM), and θ is the Bragg diffraction angle. The diffraction peaks assigned for (111) Cu_2O and (002) CuO at 36.4° and 35.5°, respectively, have been selected due to it being the highest and the most prominent crystal plane in the sample. The change in the peak intensity is related to the degree of crystallinity of the oxide layers. It is evident that CuO formation surpassing Cu_2O formation, indicating excessive formation of CuO. Although Cu_2O works well in electrochemical and photocatalytic applications, the formation of CuO compromises its stability. The irreversible redox reaction of Cu_2O is the source of this instability. This instability might be made worse by too much CuO [23]. The crystallite size for both Cu_2O and CuO increases as the annealing time increases to 180 minutes with the reading of 394.2 nm and 446.8 nm, respectively. However, the crystallite size decreases drastically to 267.9 nm and 355.8 nm for Cu_2O and Cu,O respectively, as the annealing time further increases. The sudden drop of crystallite size is because the annealing process modifies the material's strains and defects. As the annealing time increases, the lattice defects and internal stresses in the material may decrease, influencing the growth and stability of the grains [24]. This result aligns with the AFM results, which show the grain size of the Mg:Cu_2O/CuO thin films exhibits a growth trend. However, beyond a certain annealing duration, a decline in grain size is observed. This reduction is likely due to the accelerated formation and growth of CuO phases at prolonged annealing periods, which alter the microstructural characteristics of the film. The emergence of CuO, a secondary phase, can disrupt the uniform grain structure of Cu_2O and introduce new grain boundaries, leading to grain refinement and possible morphological instability [25]. This trend highlights the critical role of annealing duration in optimizing the structural and phase composition of Mg:Cu_2O/CuO thin films for optoelectronic applications.

Int. Journal of Integrated Engineering Vol. 17 No. 6 (2025) p. 210-223

3.5 Optical Properties of Interstacked Mg:Cu_2O/CuO Thin Films

Fig. 11 shows the absorption spectra for the interstacked Mg:Cu_2O/CuO thin films at various annealing times. All the samples had a similar trend of absorption spectra with an absorption edge at around 550 nm in the visible wavelength range. It is proven that all samples show strong absorption in the UV-Vis region. This is due to the fact that annealing can occasionally result in the formation of heterostructures like CuO/Cu_2O, which can improve photocurrent density and stability and improve electron-hole pair separation, which later improves their optical properties [26]. However, too much CuO thickness can impede charge transport and reduce the optical performance of the interstacked Mg:Cu_2O/CuO thin films [27-28]. It can be seen that the thin film annealed at 180 minutes obtained higher light absorption compared to the rest of the interstacked Mg:Cu_2O/CuO thin films. This can be related to the crystallite size in Fig. 5, which shows annealing at 180 minutes causes the crystallite size to grow larger. The increasing crystallite size of Cu_2O causes the absorption and emission bands to shift to longer wavelengths, called the red shift [29].

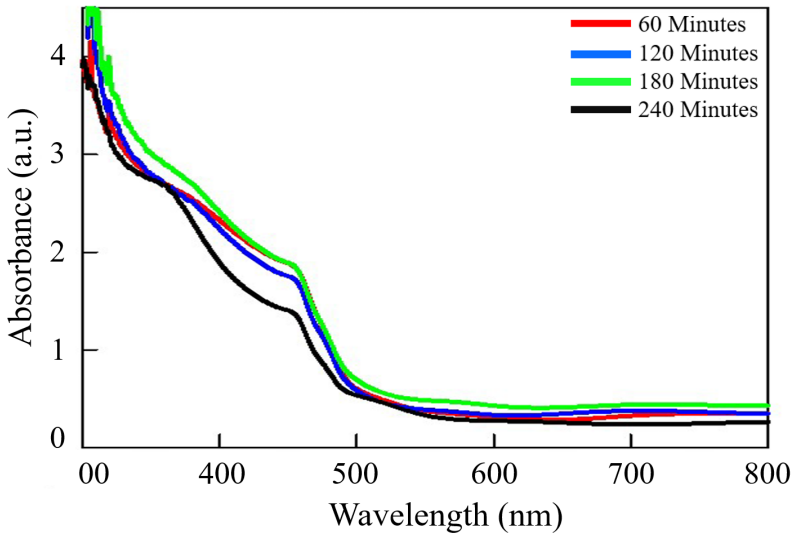

Fig. 11 *Absorption spectrum of the interstacked Mg:Cu_2O/CuO thin films*

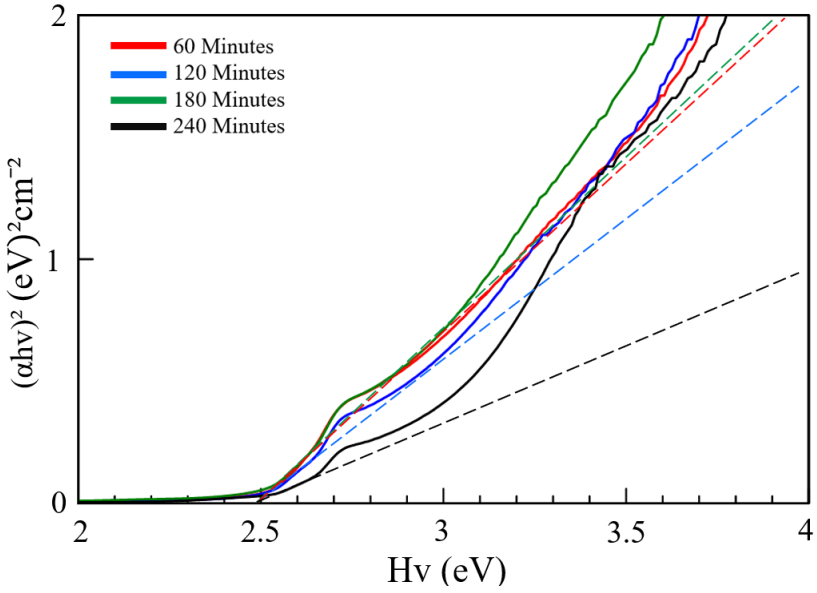

Fig. 12 *Tauc's plot for the interstacked Mg:Cu_2O/CuO thin films*

Fig. 12 displays the Tauc's plot for the interstacked Mg:Cu_2O/CuO thin films. The equation used is $(ahυ)^2 = A(hυ - Eg)^n$, where a is the absorption coefficient, υ is the photon's frequency, hυ is the photon's energy, and n is an exponential coefficient with values of 0.5 and 2 for direct and indirect electronic transitions, respectively. At 60

minutes (red line), the film exhibits a slightly higher energy onset (~2.6–2.7 eV) with a moderate slope, indicating the formation of a well-structured semiconductor layer with minimal oxidation or phase transitions. As the annealing time increases to 120 minutes (blue line), the band gap appears to decrease slightly, accompanied by a more gradual slope or tailing. This behavior may suggest the presence of increased defect states or the onset of phase mixing, possibly involving CuO [30]. The film annealed for 180 minutes (green line) shows the highest slope among all, indicating a sharper absorption edge. This is often associated with improved crystallinity and a reduction in sub-gap defect states. In contrast, the sample at 240 minutes (black line) displays a dual absorption behavior with noticeable curvature between 2.4–2.8 eV and a secondary slope beginning near 3.2 eV. This pattern suggests the coexistence of two phases, Cu_2O and CuO. The overall reduced slope and broadened transition region imply increased disorder, possible phase segregation, or oxidation-induced changes.

Tauc's plot can also be used to determine the optical band gap of the samples. The band gap energy is represented by an intercept at the hυ axis in the $(ahυ)^2$ vs hυ plot [31]. All samples achieved a constant band gap, Eg, of 2.50 eV. This finding aligns with Y. Wang et. al., who obtained a band gap of 2.51 eV after annealing. This increase is explained by the decrease in Urbach energy, which shows that defect elimination contributes to bandgap widening [32]. The band gap obtained is higher than the band gap of a pure Cu_2O, reported to be around 2.02 eV to 2.17 eV [33-34]. The difference for all samples, despite the equal band gap, is due to their variation of crystallite size as shown in Fig. 5. The sample with an annealing time of 240 minutes has the smallest crystallite size, aligned with the Tauc's plot pattern being the lowest compared to other thin films. Whilst the sample annealed at 180 minutes with the largest crystallite size exhibited the highest in Tauc's plot pattern. The optical characteristics of Cu_2O, including its absorption and emission characteristics, can change as a result of changes in crystallite size. These modifications have the potential to modify the electronic structure and, consequently, the Tauc's plot pattern [35].

3.6 Electrical Analysis of Mg:Cu_2O/CuO Thin Film

Fig. 13 shows the Hall effect measurement at room temperature used to identify the carrier concentration, mobility carrier, and resistivity of all the interstacked Mg:Cu_2O/CuO thin films. According to first principles theoretical calculations, Cu_2O is a naturally cation-deficient and intrinsically "p-type" material because of negatively charged copper vacancies [36]. The mobility carrier increases while carrier concentration decreases with respect to increasing annealing time. Annealing decreases the film's defects and non-radiative recombination centers, which typically trap carriers and limit mobility. It will also increase carrier mobility by enhancing the film's crystal quality and lowering non-radiative recombination [37]. The carrier concentration of Cu_2O films typically decreases with annealing because the high temperature reduces defect states and increases the carrier compensation effect [38]. The carrier concentration ranges between 2.255 to 2.483 x 10^{21} (/cm^3), while the mobility carrier is varied in the range of 3.102 - 3.337 x 10 (cm^2/Vs). As the annealing time increases, the samples become more resistive (resistivity varied between 8.105 - 8.294 x 10^{-5} (Ωcm).

It is interesting to note that the mobility carrier and resistivity have almost the same graph pattern. As the annealing time increases from 60 minutes to 180 minutes, the mobility carrier and resistivity also increase to a maximum reading of 3.337 x 10 (cm^2/Vs) and 8.294 x 10^{-5} (Ωcm) respectively. This can be linked to the decrease in grain boundary scattering caused by the increase in grain size in Fig. 2. It shows that annealing causes the reduction of the mobility carrier but improves the resistivity of the samples. However, at an annealing time of 240 minutes, the mobility carrier and resistivity decrease to 3.307 x 10 (cm^2/Vs) and 8.274 x 10^{-5} (Ωcm) respectively. By decreasing lattice strain and eliminating disorder from the crystal structure, annealing improves Cu_2O's crystallinity. Charge carriers can travel more freely and encounter fewer barriers on a highly ordered lattice, which lowers the probability of carrier scattering and recombination. Increased carrier mobility is a direct result of this structural order improvement [39]. Apart from that, Yuanjiang Lv et al said that annealing has the potential to raise resistivity. For instance, thin Ag-Co films annealed at 360 °C produced ultra-high resistivity due to the formation of diffusion pits that block electron transmission [40]. In contrast, certain parameters can also cause resistivity to drop, which is due to the change in crystallinity and grain size of the material [41]. As expected from the Hall effect measurement, the carrier concentration decreases as the annealing time increases [42].

Int. Journal of Integrated Engineering Vol. 17 No. 6 (2025) p. 210-223

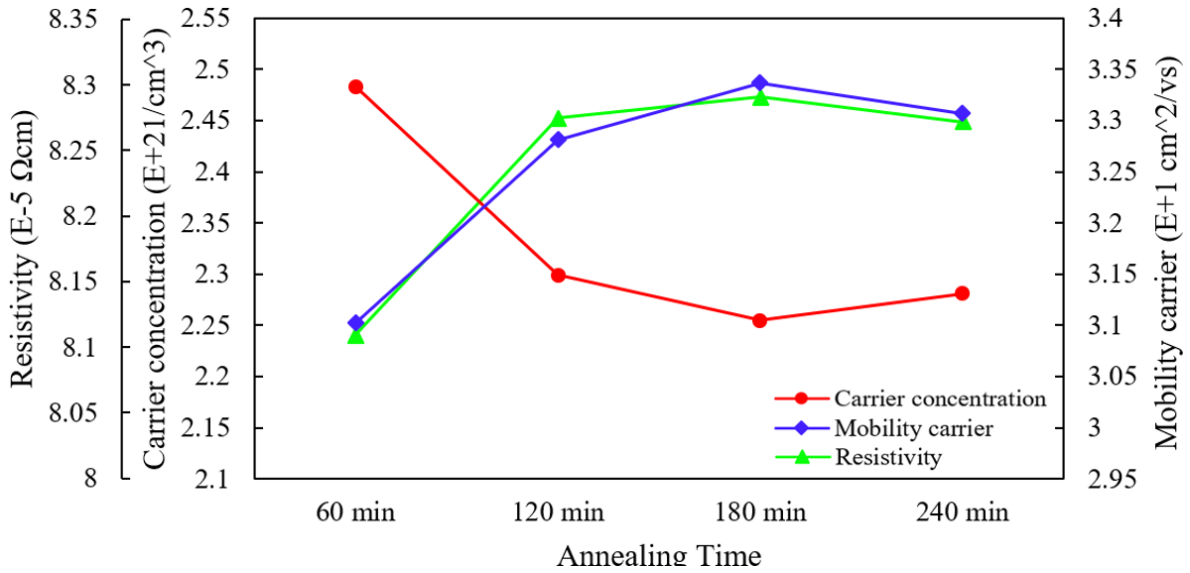

Fig. 13 *Hall effect measurements performed at room temperature for the interstacked Mg:Cu_2O/CuO thin films*

It can be seen in Fig. 8 that the carrier concentration decreases from 2.483 x 10^{21} (/cm^3) to 2.255 x 10^{21} (/cm^3) from 60 to 180 minutes of annealing time. This trend aligns with findings from previous research, indicating that as the annealing time increases, the intrinsic defects that contribute to the p-type conductivity of CuO decrease, resulting in a reduction of the carrier concentration. Due to the existence of copper vacancies (VCu), which serve as acceptor states and supply holes as charge carriers, CuO is usually a p-type semiconductor. Long-term annealing of the material, especially in an oxygen-rich environment, tends to repair these defects because more oxygen atoms diffuse into the lattice, lowering the number of copper vacancies. The carrier concentration is successfully reduced by this annealing process, which lowers the carrier density [43-44]. Apart from that, the carrier concentration increases to 2.281 x 10^{21} (/cm^3) at 240 minutes, which is most likely caused by excessive annealing that leads to excessive CuO formation, which can degrade this property [45].

4. Conclusion

This study investigated the effects of annealing time on the physical, morphological, structural, optical, and electrical properties of the interstacked Mg:Cu_2O/CuO thin films fabricated via electrodeposition, followed by annealing process. The largest Cu_2O grains were seen at 120 minutes according to morphological analysis using AFM, which showed that annealing improved grain growth and surface uniformity. Structural analysis confirmed the phase transition, revealing Cu_2O and CuO phases and an increasing CuO peak intensity with annealing time. All samples had a similar spectra trend with an absorption edge around 550 nm, confirming strong UV-Vis absorption. The band gap remained constant at 2.5 eV despite annealing, higher than pure Cu_2O due to reduced Urbach energy, indicating defect elimination widens the band gap. Hall effect measurements show that annealing time causes resistivity to increase, but reduced hole mobility compared to unannealed samples. The carrier concentration recorded was around 10^{21} cm^{-3}. However, further research and understanding regarding the Cu_2O's interface, heterojunction, and overall performance efficiency are needed.

Acknowledgement

The author gratefully acknowledges the financial support provided by the Malaysian Ministry of Higher Education (MOHE) through the Fundamental Research Grant Scheme (FRGS) under Grant No. FRGS/1/2024/TK08/UNIMAP/02/20.

Conflict of Interest

The manuscript is not being considered by any other journals and has not been published anywhere else. Every author has given their approval for the review, supports its submission, and states that they have no conflicts of interest with the manuscript.

Author Contribution

The authors confirm contribution to the paper as follows: ***study conception and design:*** *Fatin N. Afiqah, N. Nisha Razalli, M. Zamzuri;* ***data collection:*** *Fatin N. Afiqah;* ***analysis and interpretation of results:*** *M. Mahyiddin, A.F Aiman, H Jaafar, F. Mohamad;* ***draft manuscript preparation:*** *P. L. Khoo, M. Izaki. All authors reviewed the results and approved the final version of the manuscript.*

References

[1] Wu, L., Cheng, J., & Luo, J (2024) Semitransparent Cu2O Films Based on CuO Back Layer for Photoelectrochemical Water Splitting and Photovoltaic Applications, *ChemSusChem*, e202401994.

[2] Tuama, A., Abass, K., & Agam, M. (2021) Fabrication and Characterization of Cu_2O:Ag/Si Solar Cell Via Thermal Evaporation Technique, *International Journal of Nanoelectronics and Materials,* Vol. 13, No. 3, 601-614.

[3] Jawad, M.F., Ismail, R.A. & Yahea, K.Z, (2011) Preparation of nanocrystalline Cu2O thin film by pulsed laser deposition. *J Mater Sci: Mater Electron*, vol. 22, pp. 1244–1247. https://doi.org/10.1007/s10854-011-0294-0

[4] Pannan I. Kyesmen, Nolwazi Nombona, and Mmantsae Diale (2021) A Promising Three-Step Heat Treatment Process for Preparing CuO Films for Photocatalytic Hydrogen Evolution from Water, *ACS Omega 2021*, vol. 6, no. 49, pp. 33398-33408. doi: 10.1021/acsomega.1c03796

[5] Park, K. W., Gleason, K. K., & Yang, R. (2025) Advanced Morphological Control of Polymeric Surfaces Using Initiated Chemical Vapor Deposition (iCVD), *Advanced Functional Materials*, vol, 35, no. 24, pp. 2417620.

[6] Ingole, R. S., Kadam, S. L., Chavan, G. T., Kulkarni, S. B., Lokhande, B. J., & Ok, J. G. (2024) Solvent-mediated spray pyrolysis of 2D vanadium oxide nanostructures for high-performance energy storage applications. *Electrochimica Acta*, vol. 498, pp. 144628.

[7] Sajid, S., Alzahmi, S., Salem, I., & Obaidat (2022) Guidelines for Fabricating Highly Efficient Perovskite Solar Cells with Cu_2O as the Hole Transport Material, *Nanomaterials*, vol. 12, https://doi.org/10.3390/nano12193315

[8] Luo, L., Zhou, B., Liu, Z., Zhao, Q., Wang, C., Duan, et. al. (2023) Study of Se/Te-doped Cu_2O as a hole transport material in perovskite solar cells, *RSC Advances*, vol. 13, pp. 8476 - 8486, https://doi.org/10.1039/D2RA04659H

[9] Wang, L., Su, J., Guo, Y., Lin, Z., Hao, Y., & Chang, J (2021) 97.3% Pb-Reduced CsPb1-xGexBr3 Perovskite with Enhanced Phase Stability and Photovoltaic Performance through Surface Cu Doping, *The journal of physical chemistry letters*, pp. 1098-1103, doi:10.1021/acs.jpclett.0c03580

[10] Akshai S., Anand M. P., Ramesh R., NandaKumar A. K., Balaji D., et al (2025). A Comprehensive Study on the Impact of Off-Stoichiometry and Mg Doping in CuCrO2 Thin Films for Heterojunction Device Fabrication. ACS Applied Electronic Materials. https://doi.org/10.1021/acsaelm.4c01838.

[11] Arshad, Z., Khoja, A., Shakir, S., Afzal, A., Mujtaba, M., Soudagar, M., Fayaz, H., C., S., Farukh, S., & Saeed, M (2021) Magnesium-doped TiO_2 as an efficient electron transport thin film in perovskite solar cells, *Case Studies in Thermal Engineering*, vol. 26, pp. 101101, https://doi.org/10.1016/j.csite.2021.101101

[12] Usman A, Bovornratanaraks T. (2024) Modeling and Optimization of Modified TiO2 with Aluminum and Magnesium as ETL in MAPbI3 Perovskite Solar Cells: SCAPS 1D Frameworks, *ACS Omega*, 12;9(38), 39663-39672, doi: 10.1021/acsomega.4c04505

[13] A. Ringleb, R. Ruess, N. Hofeditz, W. Heimbrodt, T. Yoshida, D. Schlettwein (2021) Influence of Mg-doping on the characteristics of ZnO photoanodes in dye-sensitized solar cells, *Physical Chemistry Chemical Physics*, vol. 23, no. 14, pp. 8393-8402, http://dx.doi.org/10.1039/D1CP00179E

[14] N. M. Arifin, F. Mohamad, R. Hussin, A. Z. M. Ismail, S. A. Ramli (2023) Annealing Treatment on Homogenous n-TiO2/ZnO Bilayer Thin Film Deposition as Window Layer for p-Cu2O-Based Heterostructure Thin Film, *Coatings*, vol. 13, no. 1, pp. 206, https://doi.org/10.3390/coatings13010206

[15] K. Sahu, S. A. Khan, A. Pandey, S. Mohapatra (2021) Thermal evolution of morphological, optical, and photocatalytic properties of Au–Cu_2O–CuO nanocomposite thin film, *Journal of Materials Science: Materials in Electronics,* vol. 32, no. 19, pp. 24058-24068, doi:10.1007/s10854-021-06868-5

[16] C. Loka, K. S. Lee (2021) Preparation and photocatalytic performance of silver nanocrystals loaded Cu_2O-WO3 composite thin films for visible light-active photocatalysis, *Materials Research Bulletin,* no. 137, pp. 111192, doi: 10.1016/j.materresbull.2020.111192

[17] M. Marina, N. N. Razalli, M. Zamzuri, S. Zainal, A. R. Nani, F. Mohamad, et. al. (2021) Construction of internally stacked Cu_2O: CuO layers in Cu_2O: CuO/Gr/ZnO heterojunctions for solar cells applications, *Journal of Physics: Conference Series*, vol. 2051, no. 1, pp. 012069, 2021, doi: 10.1088/1742-6596/2051/1/012069

[18] SM Zainal, M Zamzuri, M Hasnulhadi, Z Nooraizedfiza, M Marina, F Mohamad, et. al. (2018) Effect of annealing temperature on construction of CuO layer on electrodeposited-Cu_2O layer by annealing, *IOP Conference Series: Materials Science and Engineering*, vol. 429, no. 1, pp. 012097, doi:10.1088/1757-899X/429/1/012097

[19] Skaria, G., Saikumar, A., Shivprasad, A., & Sundaram, K (2021) Annealing Studies of Copper Indium Oxide (Cu_2In_2O5) Thin Films Prepared by RF Magnetron Sputtering, *Coatings*, https://doi.org/10.3390/coatings11111290

[20] M. Benaissa, H. Si Abdelkader, G. Merad (2022) Dependence of cuprous oxide conductivity on metal doping: a hybrid density functional simulation, *The European Physical Journal B 95*, no. 5, pp. 82, https://doi.org/10.1140/epjb/s10051-022-00340-x

[21] Marina, M., Razalli, N., Zamzuri, M., Zainal, S., Nani, R., Mohamad, F., & Izaki, M (2021) Construction of internally stacked Cu_2O:CuO thin films in Cu_2O:CuO/Gr/ZnO heterojunctions for solar cells applications, *Journal of Physics: Conference Series*, pp. 2051, doi: 10.1088/1742-6596/2051/1/012069

[22] Lee, W., & Wang, X (2021) Structural, Optical, and Electrical Properties of Copper Oxide Films Grown by the SILAR Method with Post-Annealing, *Coatings*, https://doi.org/10.3390/coatings11070864

[23] Wan, L., Zhou, Q., Wang, X. et al. (2019) Cu_2O nanocubes with mixed oxidation-state facets for (photo)catalytic hydrogenation of carbon dioxide. *Nat Cata*l 2, 889–898, https://doi.org/10.1038/s41929-019-0338-z

[24] Sellaiyan, S., Devi, L., Sako, K., Uedono, A., & Sivaji, K (2019) Effect of dopant concentration and annealing of Yttrium doped CuO nanocrystallites studied by positron annihilation spectroscopy, *Journal of Alloys and Compounds,* https://doi.org/10.1016/j.jallcom.2019.02.247

[25] Khalifa, M. (2024). Cu_2O/CuO composite for efficient performance in photoelectrochemical and optoelectronics applications. *Physica Scripta,* 99. https://doi.org/10.1088/1402-4896/ad51b5

[26] Du, F., Chen, Q., & Wang, Y (2017) Effect of annealing process on the heterostructure CuO/Cu_2O as a highly efficient photocathode for photoelectrochemical water reduction, Journal of Physics and Chemistry of Solids, no. 104, pp. 139-144, doi: 10.1016/j.jpcs.2016.12.029

[27] Jeong, D., Jo, W., Jeong, J., Kim, T., Han, S., Son, M., & Jung, H (2022) Characterization of Cu_2O/CuO heterostructure photocathode by tailoring CuO thickness for photoelectrochemical water splitting, *RSC Advances*, no. 12, pp. 2632 - 2640, http://dx.doi.org/10.1039/D1RA08863G

[28] Seo, Y., Arunachalam, M., Ahn, K., & Kang, S (2021) Integrating heteromixtured Cu_2O/CuO photocathode interface through a hydrogen treatment for photoelectrochemical hydrogen evolution reaction, *Applied Surface Science*, no. 551, pp. 149375, 2021. doi: 10.1016/j.apsusc.2021.149375

[29] Gizhevskii, B., Sukhorukov, Y., Moskvin, A., Loshkareva, N., Mostovshchikova, E., Ermakov, A., et. al. (2006) Anomalies in the optical properties of nanocrystalline copper oxides CuO and Cu_2O near the fundamental absorption edge, *Journal of Experimental and Theoretical Physics,* no. 102, pp. 297-302, https://api.semanticscholar.org/CorpusID:122272775

[30] B.D. Viezbicke, S. Patel, B.E. Davis, D.P. Birnie III (2015) Evaluation of the Tauc method for optical absorption edge determination: ZnO thin films as a model system: Tauc method for optical absorption edge determination, *Phys. Status Solidi B* 252 (8), https://doi.org/10.1002/pssb.201552007

[31] Özmenteş, R. (2019) Effect of Thermal Annealing Time on The Optical Characteristics of CuO Thin Films, no. 24, pp. 176-182.

[32] Wang, Y., Miska, P., Pilloud, D., Horwat, D., Mücklich, F., & Pierson, J, (2014) Transmittance enhancement and optical band gap widening of Cu_2O thin films after air annealing, *Journal of Applied Physics*, 115, doi: 10.1063/1.4865957

[33] Malik, M., Fakhr-E-Alam, M., Aslam, S., Qureshi, M., Yunus, G., Elaimi, A., & Saleem, M (2023) Influence of Vanadium substitution on electronic, thermoelectric and optical response of Cu_2O, *Physica Scripta*, 98, doi: 10.1088/1402-4896/ad0de5

[34] Li, J., He, M., Yan, J., Liu, J., Zhang, J., & , J (2022) Room Temperature Engineering Crystal Facet of Cu_2O for Photocatalytic Degradation of Methyl Orange, *Nanomaterials,* no. 12, https://doi.org/10.3390/nano12101697

[35] N Kumar, SS Parui, S Limbu, DK Mahato, N Tiwari, RN Chauhan (2021) Structural and optical properties of sol–gel derived CuO and Cu_2O nanoparticles, *Materials Today: Proceedings*, no. 41, pp. 237-241, doi: 10.1016/j.matpr.2020.08.800

[36] Sequeda, I., & Meléndez, Á (2022) Understanding the Role of Copper Vacancies in Photoelectrochemical CO_2 Reduction on Cuprous Oxide, *The journal of physical chemistry letters*, pp. 3667-3673, https://doi.org/10.1021/acs.jpclett.2c00751

[37] Hu, M., Xu, L., Zhang, X., Hao, H., Chen, H., Song, Z., Luo, S., & Zhu, Z. (2023) High mobility amorphous InSnO thin film transistors via low-temperature annealing, *Applied Physics Letters.* https://doi.org/10.1063/5.0131595.

[38] Han, S., Niang, K., Rughoobur, G., & Flewitt, A (2016) Effects of post-deposition vacuum annealing on film characteristics of p-type Cu_2O and its impact on thin film transistor characteristics, *Applied Physics Letters*, no. 109, pp. 173502, doi: 10.1063/1.4965848

[39] Peng, W., Zhou, Y., Li, J., Liu, Y., Zhang, J., Xiang, G., Zhu, X., Li, R., Wang, H., & Zhao, Y (2021) Annealing temperature induced physical characteristics of CuO films grown by magnetron sputtering, *Materials Science in Semiconductor Processing,* no. 131, 105883, doi: 10.1016/j.mssp.2021.105883

[40] Lv, Y., Sun, H., Shi, P., Lian, X., Zhang, H., Li, S., Liang, S., Wang, G., &, F (2022) The Effect of Co Content and Annealing Temperatures on the Resistivity in Ag-Co Films, *Nanomaterials*, 12, https://doi.org/10.3390/nano12132297

[41] Kaisha, A., Caffrey, D., Ainabayev, A., Toktarbaiuly, O., Ibraimov, M., Wang, H., Nuraje, N., & Shvets, I (2024) Examining the Desirable Properties of ZnSnOy by Annealing Treatment with a Real-Time Observation of Resistivity, *ACS Omega*, no. 9, pp. 26205 - 26212, https://doi.org/10.1021/acsomega.4c01857

[42] Han, S., & Flewitt, A (2017) Analysis of the Conduction Mechanism and Copper Vacancy Density in p-type Cu_2O Thin Films, *Scientific Reports*, 7, doi: 10.1038/s41598-017-05893-x

[43] Aparicio-Huacarpuma, B., Aragon, F., Villegas-Lelovsky, L., Soncco, C., Pacheco-Salazar, D., Guerra, J., De Morais, P., Da Silva, S., & Coaquira, J (2024) Thickness dependence of the room-temperature ethanol sensor properties of Cu_2O polycrystalline films, *Nanotechnology*, 35, doi: 10.1088/1361-6528/ad47cc

[44] Seo, Y., Arunachalam, M., Ahn, K., & Kang, S (2021) Integrating heteromixtured Cu_2O/CuO photocathode interface through a hydrogen treatment for photoelectrochemical hydrogen evolution reaction, *Applied Surface Science,* 551, 149375, doi: 10.1016/j.apsusc.2021.149375

[45] Lee, H., Lee, G., Lee, H., Lee, T., Kim, I., Kim, M., Lim, B., & Koo, S (2024) Effects of Postdeposition Annealing on the Electrical Properties of Cu_2O/4H–SiC PiN Diodes, *Electronic Materials Letters*, doi: 10.1007/s13391-024-00484-1